analytical chemistry

Technical Note

Cite This: *Anal. Chem.* XXXX, XXX, XXX−XXX

pubs.acs.org/ac

Mirror Switching for High-Resolution Ion Isolation in an Electrostatic Linear Ion Trap

Joshua T. Johnson, Ian J. Carrick, Gregory S. Eakins, and Scott A. McLuckey*

Department of Chemistry, Purdue University, 560 Oval Drive, West Lafayette, Indiana 47907-2084, United States

Supporting Information

ABSTRACT: Ion isolation was achieved via selective pulsing of the entrance and exit ion mirrors in an electrostatic linear ion trap mass spectrometer (ELIT). Mirror switching has been described previously as a method for capturing injected ions in ELIT devices. After ion trapping, mirror switching can be used as a method for ion isolation of successively narrower ranges of mass-to-charge (m/z) ratio. By taking advantage of the spatial separation of ions in an ELIT device, pulsing of the entrance and/or exit mirrors can release unwanted ions while continuing to store ions of interest. Furthermore, mirror switching can be repeated multiple times to isolate ions of very similar m/z values with minimal loss of the stored ions, as is demonstrated by the isolation of protonated L-glutamine and L-lysine (Δ m/z = 0.0364) from a mixture of the two amino acid ions and the isobaric mixture of [PC P-18:0/22:6] and [PC 19:0/19:0] (Δ m/z = 0.0575). As isolation is accomplished due to the spatial/temporal separation of ion packets within the ELIT, multiple reflection-time-of-flight (MR-TOF) mass spectra are shown to demonstrate separation in the ELIT at the time of isolation. An isolation resolution of greater than 35 000 fwhm is demonstrated here using a 5.25 in. ELIT. This resolution corresponds to the fwhm resolution necessary to reduce contaminant overlap of an equally abundant adjacent ion to 1% or less of the isolated ion intensity.

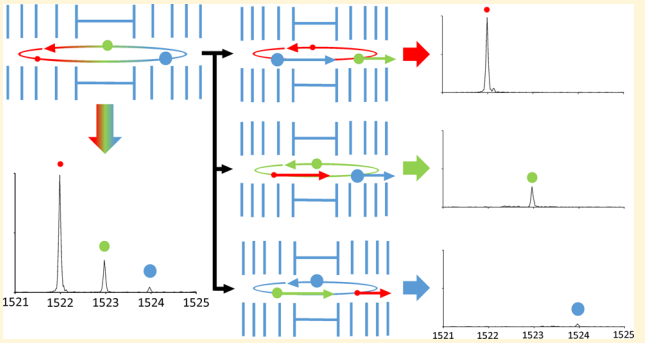

The efficiency and resolution with which precursor ions can be selected for subsequent interrogation are important figures of merit in any tandem mass spectrometry (MS/MS) experiment.[1] Various precursor ion selection approaches have been used in the many MS/MS platforms that have been developed over the past several decades. A particularly common approach in many commercial platforms, for example, is the use of a quadrupole mass filter for precursor ion isolation. In the case of most tandem time-of-flight (TOF/TOF) instruments, a single-pass TOF process is used to separate precursor ions for subsequent activation.[2] Improved precursor ion resolution can be achieved via multiple reflection TOF (MR-TOF) via a significant extension in ion flight path, as demonstrated with the commercially available spiralTOF, an open-path MR-TOF/TOF mass spectrometer that offers a fixed path length of 17 m for precursor ion isolation and a single reflection TOF for mass analysis.[3,4]

A high degree of selectively in ion flight length can be achieved via ion storage time in a closed-loop MR-TOF device.[5] After a given storage time, ions can be released for detection or to an external device for subsequent processing. A deflector, such as a Bradbury-Nielsen gate, is commonly used to selectively pass ions within a small m/z range after a MR-TOF separation.[6−12] Similarly, isolation by in-trap potential lift ejection has also been demonstrated.[13] Alternatively, a trapping plate can be modulated such that unwanted ions become unstable over time to accomplish ion isolation within MR-TOF devices.[14,15] Recently, authors using a MR-TOF device with a single in-trap deflector consisting of two electrodes quoted an ion selection resolution of 40,000 using square wave modulation using low voltages.[16,17] Ions can also be selectively retrapped in an injection region then sequentially reinjected into the MR-TOF.[18] Isolation is accomplished due to the small acceptance window of the retrapping field. Using this technique isolation, resolutions up to 70 000 were quoted with trapping efficiencies of up to 35%.

The electrostatic linear ion trap (ELIT), which consists of two ion mirrors facing each other and separated by a field free region, is a common platform for MR-TOF measurements.[19−21] The linear geometry is convenient for ion isolation because ion injection and release can occur via the same ion mirror or via opposite mirrors. Ions are introduced axially at a fixed energy and are trapped between the two ion mirrors. Although there is no inherent limit to the m/z values that can be trapped in an ELIT device, the physical dimensions of the trap and trapping method (e.g., mirror switching[22] or potential lift[13,23−25]) limit the maximum achievable mass range for a given injection of ions. It has been demonstrated, however, that use of multiple injection events can be used to partially overcome this

Received: February 16, 2019
Accepted: June 17, 2019
Published: June 17, 2019

DOI: 10.1021/acs.analchem.9b00874
Anal. Chem. XXXX, XXX, XXX−XXX

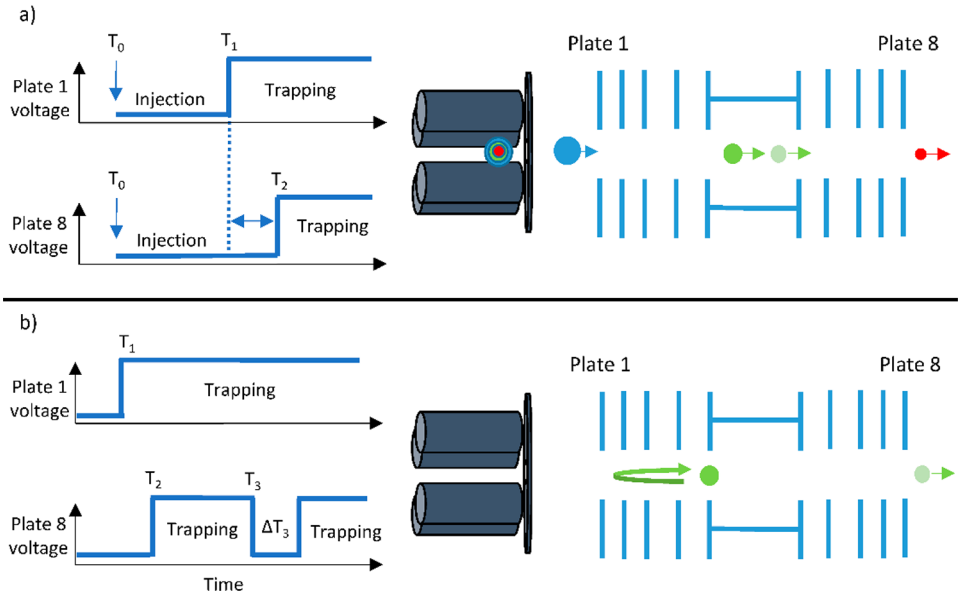

Figure 1. Illustration of techniques used in mirror switching isolation. (a) Selection of a restricted mass range by pulsing plates 1 (T_1) and 8 (T_2) after ion injection (T_0). (b) High-resolution ion selection after adequate separation time using a third pulse (T_3) of a given width (ΔT_3).

limitation.[17] Mass analysis can be achieved via MR-TOF using an external detector following release from the ELIT or Fourier transform mass spectrometry (FTMS),[26] using a pick-up electrode within the ELIT for image current detection, or both.[27] A serious potential complication for both mass analysis and ion isolation using a closed-path MR-TOF device, however, is the so-called "race track effect"[28] whereby fast ions lap slow ions leading to ambiguity in mass selection/determination. Herein, we describe and demonstrate a general approach to achieving high-resolution (>10 000) ion isolation with high efficiency (i.e., little or no ion loss) using multiple mirror switching pulses with an ELIT. Isolation resolution is defined here as the full width at half-maximum (fwhm) resolution necessary to reduce peak overlap from an equally abundant adjacent ion to 1% or less of the amplitude of the ion of interest. This approach has been implemented on an ELIT of relatively modest length (5.25 in.) but applies to any closed-loop MR-TOF device.

EXPERIMENTAL SECTION

Materials. L-Lysine monohydrochloride, L-glutamine, and ammonium acetate were purchased from Sigma-Aldrich (St. Louis, MO). [PC P-18:0/22:6] and [PC 19:0/19:0] were purchased from Avanti Polar Lipids (Alabaster, AL). Methanol was purchased from Thermo Fisher Scientific (Waltham, MA). HPLC-grade water was purchased from Fisher Scientific (Pittsburgh, PA). The LC/MS tuning mix for ESI (G2421A) was purchased from Agilent Technologies (Santa Clara, CA). The mixture of L-lysine (100 μM) and L-glutamine monohydrochloride (1 mM) was prepared using 50/50 v/v MeOH/H_2O. The mixture of [PC P-18:0/22:6] (100 μM) and [PC 19:0/19:0] (100 μM) was prepared using 99/1 v/v MeOH/1 mM ammonium acetate.

Mass Spectrometry. All experiments were carried out on a home-built 5.25 in. ELIT that has been described previously.[27] The nanoelectrospray ionization (nESI) source and the method by which ions are concentrated and injected into the ELIT have been described previously, and a brief description is provided in the Supporting Information.[29] Procedures for obtaining mass spectra via Fourier transformation and via MR-TOF with this device have been described,[25] and a summary is provided in the Supporting Information. It is important to note that the MR-TOF spectra shown here provide an estimate of the time separation of the ions in the ELIT at the time of ejection; however, peaks are broadened due to the mirror foci (temporal focusing) being at the center of the trap for FT measurements and not at the face of the MCP.

Ion Isolation. Ion isolation was performed by pulsing of the first plate of the ELIT (plate 1) or the last plate (plate 8) (or both) from their nominal trapping potentials (~2360 V) to ground at some specified time after ion injection. It is important to note that the voltage necessary for ion ejection needs only to be lower than the nominal ion energy (~1960 eV/charge). The time in which the electrodes are pulsed and the duration they are held at ground was set by a pulse/delay generator (model 575, Berkeley Nucleonics, San Rafael, CA). A home-built digital signal joiner was developed for combining waveforms from multiple signal sources such that a single mirror could be pulsed multiple times by coupling up to three input TTL signals. This device allowed for high accuracy control over multiple mirror switching events using the BNC 575 pulse/delay generator. Each signal drives a high impedance input that prevents interference or signal degradation of adjacent channels. By utilizing high-speed CMOS technology, the circuit was configured such that the propagation delay stays within an 8.5 ns window. Mirror switching was done using ORTEC 556 power supplies and solid-state switches (HTS 31-03-GSM, Behlke Electronics GMBH, Kronberg, Germany).

RESULTS AND DISCUSSION

In an ELIT device, ions separate in time until some maximum separation is achieved based on the relative ion velocities and dimensions of the mass analyzer, after which fast ions overtake slow ions (i.e., the race track effect). The race track effect must be avoided to achieve ion isolation without contamination due to ion lapping. For the separation of ions of very similar m/z ratio, long flight times/distances are required. It is therefore important to be able to dynamically control the m/z range of the

DOI: 10.1021/acs.analchem.9b00874
Anal. Chem. XXXX, XXX, XXX−XXX

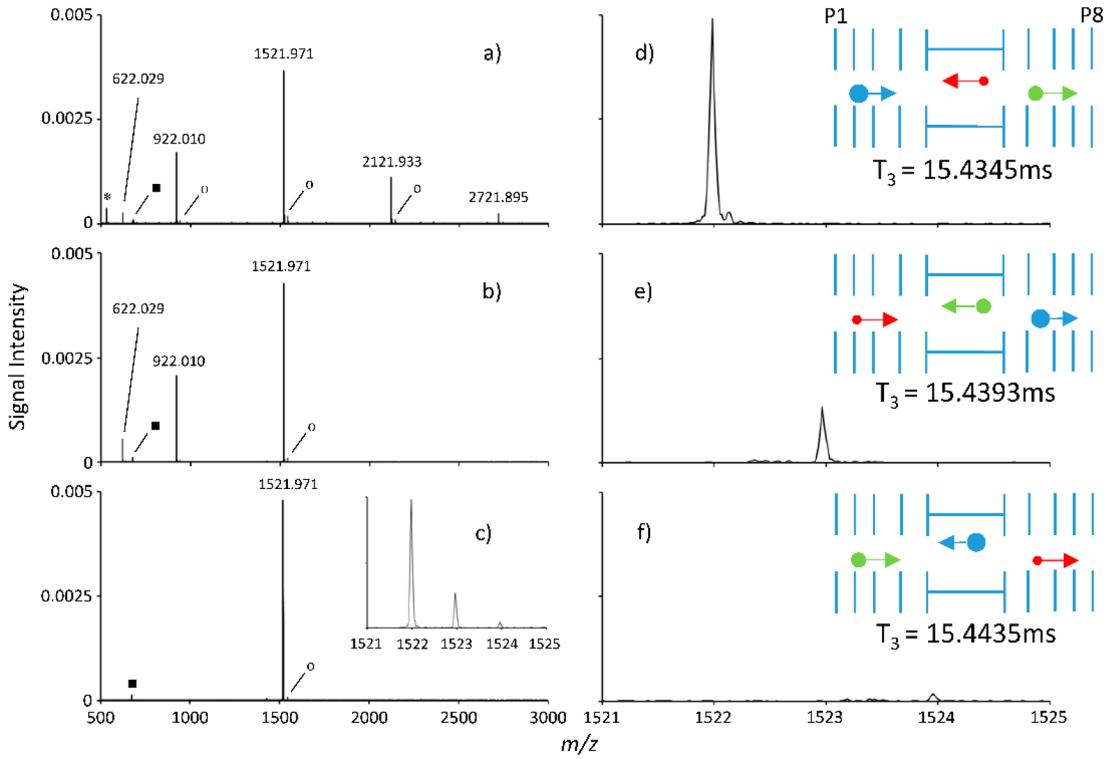

Figure 2. eFT mass spectra of Agilent ESI tuning mix. (a) Tuning mix with wide m/z range acceptance (T_1 = 20 μs). (b) Reduction of the m/z range at the high end by use of T_1 = 13.5 μs. (c) Isolation of 1521.97 peak and its isotopes by use of T_1 = 13.5 μs (plate 1) and T_2 = 19 μs (plate 8). (d–f) Isolation of successive isotopes at different T_3 values (96.7% efficient) (see inserts). Intensity scales are the same for each eFT spectra, and efficiencies are within the experimental reproducibility for this device. All mass spectra are averages of 100 spectra. All transients are 300 ms in length. The * indicates background noise. The ○ represents sodiated peaks. The ■ represents peaks associated with harmonics.

ions stored in the ELIT, which can be achieved via the appropriately timed release of ions that might otherwise lap or be lapped by the ions of interest. By progressively reducing the range of masses trapped in the device, high spatial separation can be achieved for ions of very similar m/z ratios, as illustrated schematically in Figure 1 for a simple four-component mixture. The accepted m/z range for an ion population released from the accumulation ion trap at T_0 in the present device is determined by the timing of raising the voltage applied to plate 1 (entrance mirror) from 0 V to the value used to store ions at T_1.[25] High m/z ions too slow to enter the ELIT prior to T_1 are precluded from being trapped and low m/z ions that bounce from the opposing mirror (plate 8) and exit through plate 1 before T_1 are also precluded from being trapped. The ions at the lower end of the trapped m/z range can begin to lap the ions at the upper end of the m/z range after the low m/z ions have undergone a single lap. To avoid such a scenario, it is desirable to limit the initial m/z range of trapped ions to allow for ions to separate in time while avoiding any ion lapping. It is straightforward to restrict the m/z range of trapped ions in the initial ion injection step (i.e., a low resolution selection step) by using two timed mirror switches, as illustrated in Figure 1a. One of several ways to do this is to time the gating of plates 1 and 8 such that only ions with flight times between the two gates pulse are stored. In the schematic of Figure 1a, plate 1 is gated up at T_1 to prevent (blue) ions of m/z higher than those of interest from entering the trap while plate 8 is gated up at T_2 just before the ions of interest can exit, thereby allowing faster (red), lower m/z ions to pass through the trap. The trapped (green) ions of a relatively narrow m/z range can then be allowed to further separate in time to the point at which another mirror switch at T_3 with a given pulse width (ΔT_3) can be used to allow unwanted (lighter green) ions to escape the ELIT. This is illustrated in Figure 1b.

The initial mass selection step illustrated in Figure 1a, in which T_1 determines the high m/z cutoff and T_2 determines the low m/z cutoff, is relatively crude because it depends on the degree of separation that takes place during the short time-of-flight associated with the initial injection step from the trapping quadrupole. Nevertheless, it prevents the immediate onset of ion lapping when ions of widely different m/z values are initially stored in the ELIT. The unlapped m/z-range in a MR-TOF, expressed as the ratio of the upper $(m/z)_{max}$ and lower $(m/z)_{min}$ m/z limits, is approximated by[30]

$$\frac{(m/z)_{max}}{(m/z)_{min}} \approx \left(\frac{N+1}{N}\right)^2 \quad (1)$$

Based on this relationship, it is possible to estimate the number of laps (N), as determined by the storage time, that can be allowed before the ions in the initially selected ion population can begin to undergo ion lapping:

$$N \approx \left(\left(\frac{(m/z)_{max}}{(m/z)_{min}}\right)^{1/2} - 1\right)^{-1} \quad (2)$$

At any point prior to the time that ion lapping can occur, one or more subsequent mirror switching events can be used to release unwanted ions in a selective fashion. A series of appropriately timed mirror switches can be used to provide precursor isolation at a resolution related to the temporal/spatial separation obtainable via a MR-TOF experiment. Isolation performance can also be impacted by the speed with which the

DOI: 10.1021/acs.analchem.9b00874
Anal. Chem. XXXX, XXX, XXX−XXX

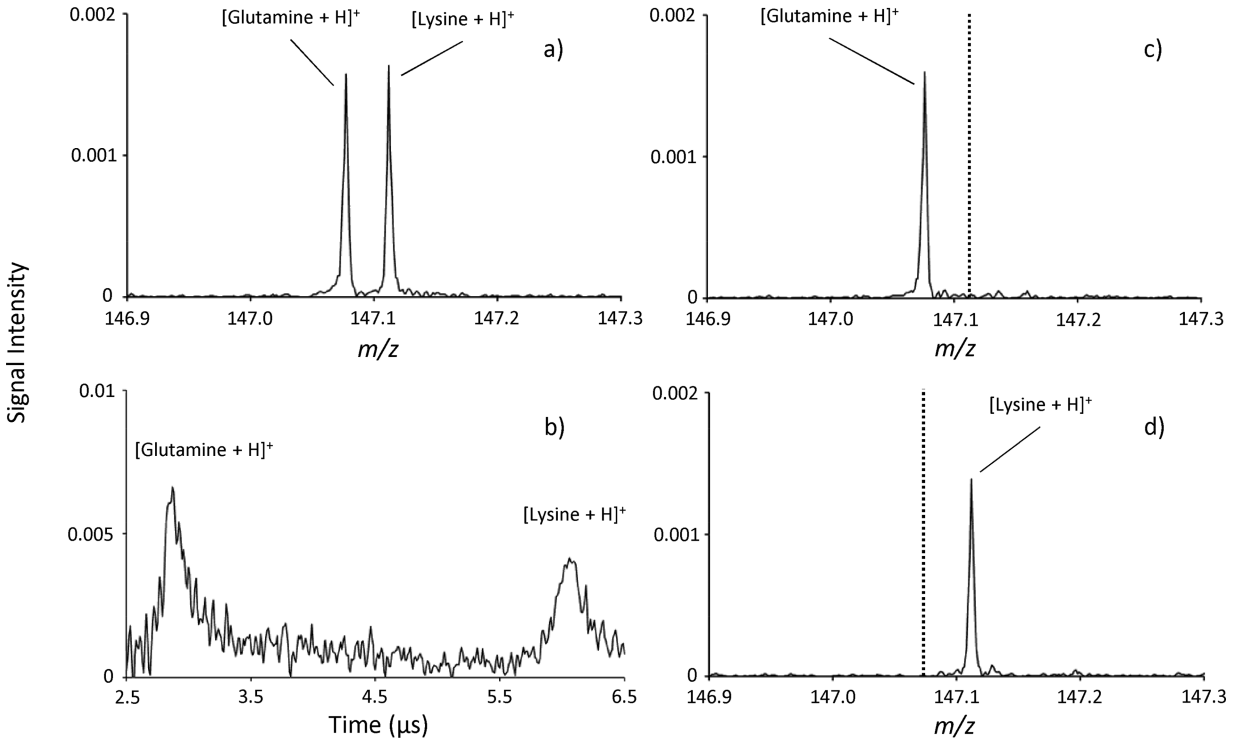

Figure 3. eFT mass spectra and MR-TOF of protonated L-glutamine (147.0764 m/z) and L-lysine (147.1128 m/z). (a) Preisolation eFT mass spectrum. (b) MR-TOF spectrum of protonated L-glutamine (left) and L-lysine (right) after 25.65 ms. (c) Isolated L-glutamine (101% efficient) after 25.65 ms. (d) Isolated L-lysine (85.9% efficient) after 25.65 ms using isolation pulse widths of 1.5 μs. Intensities scales are the same for all eFT spectra and efficiencies are within the experimentally reproducibility for this device. All mass spectra are averages of 100 spectra. All transient are 200 ms in length.

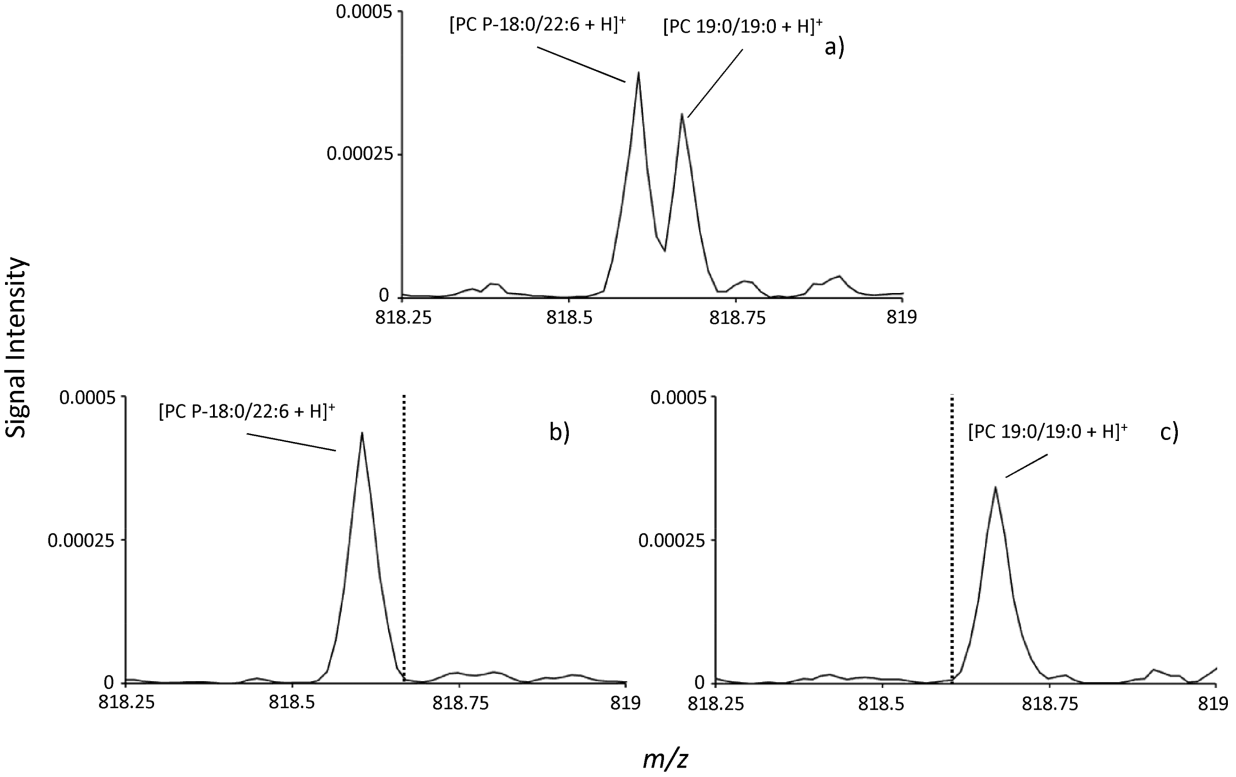

Figure 4. eFT mass spectra of protonated [PC P-18:0/22:6] (818.6063 m/z) and [PC 19:0/19:0] (818.6638 m/z). (a) eFT mass spectrum of the monoisotopic isolation of the two isobaric ions. (b) Isolated [PC P-18:0/22:6] (111% efficient) and (c) isolated [PC 19:0/19:0] (106% efficient) after 45.58 ms using a 2 μs pulse of plate 8. Intensities scales are the same for all eFT spectra, and efficiencies are within the experimentally reproducibility for this device. All eFT mass spectra are averages of 100 spectra. All transients are 300 ms in length.

DOI: 10.1021/acs.analchem.9b00874
Anal. Chem. XXXX, XXX, XXX−XXX

mirror electrodes can be switched and any associated ringing, which has been discussed for the present apparatus and is shown experimentally in Figure S-2.[25,27]

An ion isolation process for ions derived from the Agilent tuning mix is illustrated in Figure 2. The enhanced Fourier transform (eFT) mass spectrum of the tuning mix obtained after a single mirror switching event for plate 1 (T_1 = 20 μs) is shown in Figure 2a. Figure 2b shows the spectrum obtained using T_1 = 13.5 μs, which prevents the higher m/z ions from entering the ELIT. Figure 2c shows the mass spectrum obtained using a plate 1 mirror switch at T_1 = 13.5 μs and a plate 8 mirror switch at T_2 = 18.5 μs. This process prevents the higher m/z ions from entering the ELIT while it allows the lower m/z ions to pass through the ELIT. The time-of-flight separation in the single pass through the ELIT is insufficient for the isolation of the isotopologues of protonated hexakis(1H,1H,5H-octafluoropentoxy)phosphazine (monoisotopic ion = m/z 1521.971). During the storage time between T_2 and T_3 (15.47 ms and 761 laps), the isotopologues separate further such that they are spaced roughly 5 μs apart in flight time (see MR-TOF mass spectrum in Figure S-1). A third, 12 μs long mirror switch (plate 8) to ground (i.e., T_3) can be used to release two of the three isotopic peaks (d–f) remaining in the ELIT. For example, at T_3 = 15.43 ms, the locations of the isotopes in the trap are such that the two heavier isotopes are in line to reach plate 8 before the lightest isotope (see insert to Figure 2d) such that the 12 μs plate 8 pulse to ground is sufficiently long to release the two heavier isotopic ions. The order in which the three isotopic peaks reach plate 8 can be adjusted via T_3, thereby allowing for the selective release of two of the three isotopic ions (see also the insets to Figure 2e,f). The isolation resolution demonstrated for Figure 2d–f is approximately 3 700 fwhm based on the resolution necessary to reduce peak overlap to 1% of the ion of interest. (We assume a Gaussian peak shape, which approximates the shapes of the peaks we generally observe in the MR-TOF experiment.) The ion path length in the 5.25 in. ELIT was estimated to be 124 mm using a simulated model of the device in SIMION v8.1 (Scientific Instrument Services, Ringoes, NJ). A trapping time of 15.47 ms in the 5.25 in. ELIT results in 761 laps for ions of m/z 1521.971 (lap time ≈ 20.3 μs) and a time-of-flight path length of 188.7 m prior to isolation.

Higher resolution ion isolations can be achieved by allowing longer separation times for closely spaced ions. This was demonstrated with a mixture of protonated L-lysine and L-glutamine, two isobaric species that are separated by m/z 0.0364 (Figure 3), and protonated [PC P-18:0/22:6] and [PC 19:0/19:0], which are also isobaric and are separated by m/z 0.0575 (Figure 4). As can be seen with the MR-TOF spectrum of the amino acid mixture near the isolation time, the ion packets for protonated L-lysine and L-glutamine are well separated in MR-TOF space (Figure 3b). Temporal and spatial separation demonstrated in the MR-TOF measurement allowed an experimental isolation resolution of at least 10 000 fwhm (i.e., the resolution needed to isolate one of the roughly equally abundant isobaric ions with less than 1% abundance of the other isobaric ion present after the isolation step) as illustrated in panels c and d in Figure 3. Ions underwent 4071 laps after the 25.65 ms separation time (lap time ≈ 6.3 μs) and thus had a final time-of-flight path length of 1009.6 m before ion isolation. Isolation resolutions of 38 000 fwhm were achieved for a fatty acid mixture of [PC P-18:0/22:6] and [PC 19:0/19:0] (Figure 4) after 48.58 ms of separation time (lap time ≈ 14.9 μs). After 3375 laps, ions experienced a final time-of-flight length of 837.0 m before isolation.

CONCLUSIONS

A novel ion isolation approach is demonstrated here with a device capable of MR-TOF and FT mass analysis. This isolation technique takes advantage of the spatial separation possible in a closed path MR-TOF device. The range of masses trapped within an ELIT is decreased successively to allow ions of very similar m/z to separate while avoiding the race track effect. In this work, ion isolation was demonstrated to different extents on Agilent ESI tuning mix, a mixture of two closely spaced amino acids (L-glutamine and L-lysine, Δ m/z = 0.0364), and a mixture of two isobaric fatty acids ([PC P-18:0/22:6] and [PC 19:0/19:0], Δ m/z = 0.0575). Furthermore, MR-TOF mass spectra were used to demonstrate the degree of spatial/temporal separation accomplished with a 5.25 in. ELIT. This spatial separation is due to the long flight paths achievable with a closed-loop trapping device and is related to the resolution with which ions of similar m/z can be isolated from one another. In all cases reported here, flight paths of greater than 100 m were achieved using a 13.33 cm (5.25 in.) long ELIT device. In the most extreme case, a path length of 1009.6 m was achieved. Mirror switching is demonstrated as a straightforward and effective method for high-resolution and high-efficiency ion isolation in an ELIT without the incorporation of any supplemental electrical elements, such as deflection plates.

ASSOCIATED CONTENT

Supporting Information

The Supporting Information is available free of charge on the ACS Publications website at DOI: 10.1021/acs.analchem.9b00874.

Additional text describing our mass analysis procedures for both FT and MR-TOF data and a figure supporting the separation of isotopes in the isolated Agilent tuning mix distribution (PDF)

AUTHOR INFORMATION

Corresponding Author

*Phone: (765) 494-5270. Fax: (765) 494-0239. E-mail: mcluckey@purdue.edu.

ORCID

Scott A. McLuckey: 0000-0002-1648-5570

Notes

The authors declare no competing financial interest.

ACKNOWLEDGMENTS

This work was supported by the National Science Foundation NSF Grant CHE-1708338. We thank Mark Carlsen, Randy Replogle, Phil Wyss, Tim Selby, and Ryan Hilger of the Jonathan Amy Facility for Chemical Instrumentation for helpful discussions and their help with construction of the mass spectrometer. We also acknowledge Mircea Guna, Dr. James W. Hager, and Dr. Eric Dziekonski of AB Sciex for helpful discussions, data analysis software, and for providing the collision cell with a linear accelerator (LINAC).

REFERENCES

(1) Gross, J. H. *Mass Spectrometry: A Textbook*, 2nd ed.; Springer: New York, 2011; pp 415–478.

DOI: 10.1021/acs.analchem.9b00874
Anal. Chem. XXXX, XXX, XXX–XXX

(2) Schey, K.; Cooks, R.; Grix, R.; Wollnik, H. *Int. J. Mass Spectrom. Ion Processes* **1987**, *77*, 49−61.
(3) Satoh, T.; Tsuno, H.; Iwanaga, M.; Kammei, Y. *J. Am. Soc. Mass Spectrom.* **2005**, *16*, 1969−1975.
(4) Satoh, T.; Sato, T.; Tamura, J. *J. Am. Soc. Mass Spectrom.* **2007**, *18*, 1318−1323.
(5) Okumura, D.; Toyoda, M.; Ishihara, M.; Katakuse, I. *J. Mass Spectrom.* **2004**, *39*, 86−90.
(6) Bradbury, N. E.; Nielsen, R. A. *Phys. Rev.* **1936**, *49*, 388.
(7) Plaß, W. R.; Dickel, T.; Czok, U.; Geissel, H.; Petrick, M.; Reinheimer, K.; Scheidenberger, C.; Yavor, M. I. *Nucl. Instrum. Methods Phys. Res.B* **2008**, *266*, 4560−4564.
(8) Toker, Y.; Altstein, N.; Aviv, O.; Rappaport, M.; Heber, O.; Schwalm, D.; Strasser, D.; Zajfman, D. *J. Instrum.* **2009**, *4*, P09001.
(9) Plaß, W. R.; Dickel, T.; Scheidenberger, C. *Int. J. Mass Spectrom.* **2013**, *349*, 134−144.
(10) Wolf, R.N.; Beck, D.; Blaum, K.; Bohm, C.; Borgmann, C.; Breitenfeldt, M.; Herfurth, F.; Herlert, A.; Kowalska, M.; Kreim, S.; Lunney, D.; Naimi, S.; Neidherr, D.; Rosenbusch, M.; Schweikhard, L.; Stanja, J.; Wienholtz, F.; Zuber, K. *Nucl. Instrum. Methods Phys. Res. A* **2012**, *686*, 82−90.
(11) Wolf, R.N.; Wienholtz, F.; Atanasov, D.; Beck, D.; Blaum, K.; Borgmann, C.; Herfurth, F.; Kowalska, M.; Kreim, S.; Litvinov, Y. A.; Lunney, D.; Manea, V.; Neidherr, D.; Rosenbusch, M.; Schweikhard, L.; Stanja, J.; Zuber, K. *Int. J. Mass Spectrom.* **2013**, *349*, 123−133.
(12) Plaß, W. R; Dickel, T.; San Andres, S. A.; Ebert, J.; Greiner, F.; Hornung, C.; Jesch, C.; Lang, J.; Lippert, W.; Majoros, T.; Short, D.; Geissel, H.; Haettner, E.; Reiter, M. P; Rink, A.-K.; Scheidenberger, C.; Yavor, M. I *Phys. Scr.* **2015**, *2015*, 014069.
(13) Wienholtz, F.; Kreim, S.; Rosenbusch, M.; Schweikhard, L.; Wolf, R. *Int. J. Mass Spectrom.* **2017**, *421*, 285−293.
(14) Hilger, R. T.; Santini, R. E.; McLuckey, S. A. *Int. J. Mass Spectrom.* **2014**, *362*, 1−8.
(15) Hilger, R. T.; Santini, R. E.; McLuckey, S. A. *Anal. Chem.* **2013**, *85*, 5226−5232.
(16) Fischer, P.; Knauer, S.; Marx, G.; Schweikhard, L. *Rev. Sci. Instrum.* **2018**, *89*, 015114.
(17) Fischer, P.; Marx, G.; Schweikhard, L. *Int. J. Mass Spectrom.* **2019**, *435*, 305−314.
(18) Dickel, T.; Plaß, W. R.; Lippert, W.; Lang, J.; Yavor, M. I.; Geissel, H.; Scheidenberger, C. *J. Am. Soc. Mass Spectrom.* **2017**, *28*, 1079−1090.
(19) Wollnik, H.; Przewloka, M. *Int. J. Mass Spectrom. Ion Processes* **1990**, *96*, 267−274.
(20) Benner, W. H. *Anal. Chem.* **1997**, *69*, 4162−4168.
(21) Zajfman, D.; Heber, O.; Vejby-Christensen, L.; Ben-Itzhak, I.; Rappaport, M. L.; Fishman, R.; Dahan, M. *Phys. Rev. A: At., Mol., Opt. Phys.* **1997**, *55*, R1577−R1580.
(22) Dziekonski, E. T.; Santini, R. E.; McLuckey, S. A. *Int. J. Mass Spectrom.* **2016**, *405*, 1−8.
(23) Wolf, R. N.; Marx, G.; Rosenbusch, M.; Schweikhard, L. *Int. J. Mass Spectrom.* **2012**, *313*, 8−14.
(24) Knauer, S.; Fischer, P.; Marx, G.; Schabinger, B.; Schweikhard, L.; Wolf, R. *Int. J. Mass Spectrom.* **2017**, *423*, 46−53.
(25) Dziekonski, E. T.; Johnson, J. T.; Hilger, R. T.; McIntyre, C. L.; Santini, R. E.; McLuckey, S. A. *Int. J. Mass Spectrom.* **2016**, *410*, 12−21.
(26) Ring, S.; Pedersen, H. B.; Heber, O.; Rappaport, M.; Witte, P.; Bhushan, K.; Altstein, N.; Rudich, Y.; Sagi, I.; Zajfman, D. *Anal. Chem.* **2000**, *72*, 4041−4046.
(27) Dziekonski, E. T.; Johnson, J. T.; Lee, K. W.; McLuckey, S. A. *Anal. Chem.* **2017**, *89*, 10965−10972.
(28) Schury, P.; Ito, Y.; Wada, M.; Wollnik, H. *Int. J. Mass Spectrom.* **2014**, *359*, 19−25.
(29) Hilger, R. T.; Dziekonski, E. T.; Santini, R. E.; McLuckey, S. A. *Int. J. Mass Spectrom.* **2015**, *378*, 281−287.
(30) Yavor, M. I.; Plaß, W. R.; Dickel, T.; Geissel, H.; Scheidenberger, C. *Int. J. Mass Spectrom.* **2015**, *381*, 1−9.

DOI: 10.1021/acs.analchem.9b00874
Anal. Chem. XXXX, XXX, XXX−XXX